# Synchrotron 3D characterization of arrested fatigue cracks initiated from small tilted notches in steel

P. Lorenzino, J.-Y. Buffiere
*INSA-Lyon MATEIS CNRS UMR 5510*
*pablo.lorenzino@insa-lyon.fr, jean-yves.buffiere@insa-lyon.fr*

S. Okazaki, H. Matsunaga, Y. Murakami
*Kyushu University*
*okazaki.saburo.983@s.kyushu-u.ac.jp, matsunaga.hisao.964@m.kyushu-u.ac.jp, murakami.yukitaka.600@m.kyushu-u.ac.jp*

H. Matsunaga
*International Institute for Carbon-Neutral Energy Research*
*matsunaga.hisao.964@m.kyushu-u.ac.jp*

**ABSTRACT.** High resolution synchrotron X-ray tomography has been used to obtain 3D images of arrested cracks initiated at small artificial defects located on the surface of cylindrical steel specimens subjected to mode I fatigue loading. These defects consist in small semi-circular slits tilted at 0°, 30° or 60° with respect to the plane normal to the loading axis; all of them had the *same defect size,* $\sqrt{area}$ = 188 μm, where the *area* denotes the area of the domain defined by projecting the defect on a plane normal to the loading axis. Arrested cracks initiated from the notch were observed for all tilt angles at the surface of samples cycled at the fatigue limit (stress amplitude at which the specimen does not fail after $1\times10^7$ cycles).
High resolution synchrotron X-ray tomography has been used to obtain 3D images of those small defects and non-propagating cracks (NPC). Despite the fact that steel is a highly attenuating material for X rays, high resolution 3D images of the cracks and of the initiating defects were obtained (0.65 μm voxel size). The values of surface crack length measured by tomography are the same as those obtained by optical microscope measurements. The $\sqrt{area}$ values present the same tendency as the surface length of NPC, i.e. larger non-propagating cracks areas were observed in the softer steel. In the extreme case of 60º tilted defect, the crack fronts appear much more discontinuous with several cracks propagating in mode I until arrest.

**KEYWORDS.** X-ray Tomography; Notch; Arrested crack; 3D.

## INTRODUCTION

In a previous work we reported an experimental test campaign that was carried out in order to clarify the effect of defect orientation on the fatigue limit of three types of steels; JIS-S15C, JIS-S45C and JIS-SNCM439 [1]. The average Vickers hardness HV of each material measured with a load of 9.8 N was 117, 186 and 293, respectively. A semi-circular slit or hole was introduced into a cylindrical specimen with a diameter of 7 mm by electro-discharge machining or drilling. The slits were tilted at 0° 30° or 60° with respect to the plane normal to the loading axis, but all of them had the

same defect size, $\sqrt{area}$ = 188 μm, where the $\sqrt{area}$ denotes the square root of the size of projection of the defect on a plane normal to the loading axis. Fully reversed tension-compression fatigue tests were carried out at a test frequency of 150 Hz. The fatigue limit $\sigma_{FL}$ was determined as the stress amplitude at which the specimen does not fail after $1\times10^7$ cycles. For every material and notch tilt angle a non-propagating crack was found at the fatigue limit.
After performing fatigue tests, and carrying out fatigue crack propagation studies, the following conclusions were obtained:

- In JIS-S15C and JIS-S45C, the fatigue limits were nearly independent of the tilting angle, and were found in good agreement with the predicted values by the $\sqrt{area}$ parameter model [1-2]. On the other hand, in JIS-SNCM439, the fatigue limit was also in agreement with the prediction at the tilting angle of 0°, but it increased with an increase in the tilting angle.
- As shown on Fig. 1, a typical growth behavior of small crack was observed irrespective of the tilt angle; when the stress amplitude was slightly above the fatigue limit, the growth first decelerated to a certain crack length, and then started accelerating with fatigue cycles until the final failure.

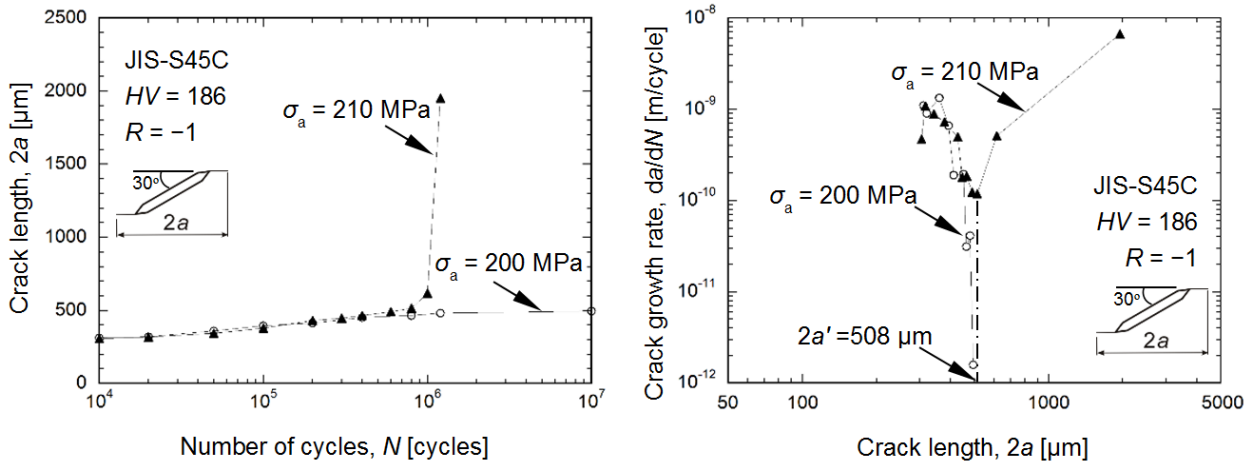


(a) (b)

Figure 1: Propagating and non-propagating cracks found above and below the fatigue limit in case of JIS S45C steel and 30° notch (a) crack length vs. number of cycles (b) Crack growth rate vs. crack length.

- The length of non-propagating cracks varied greatly according to the steel types, i.e. longer non-propagating cracks were observed in softer steel. The crack length measured at the surface was also found to be independent of the tilting angle in the case of JIS-S15C and JIS-S45C, whereas in the case of JIS-SNCM439, the length increased with an increase in the tilting angle.
- The observed crack paths were in good agreement with the direction normal to the maximum principle stress near the defect (2D analysis).

To complement the information reported above and understand the phenomenon in more detail, it was noted that further investigation was needed to clarify the three dimensional shapes of the non-propagating cracks.
As a step forward in this direction, this paper shows 3D experimental characterization of the non-propagating fatigue cracks using high resolution X-ray tomography.

## EXPERIMENTAL

### *Specimens*

In order to perform the X-ray analysis of non-propagating fatigue cracks, a smaller specimen with a square cross-section ranging from 0.8 to 1 mm² was cut from the larger sample, such that it contained the notch and the non-propagating fatigue crack. As the cross sectional area of the small samples cannot be larger than 1 mm² due to experimental restrictions and some of the samples contained cracks measuring up to 700 μm in surface length, extreme care was taken when cutting the sample. The procedure consisted in extracting a larger sample containing the notch plus crack and then applying successive steps of polishing and microscope observation until the final geometry was reached.

Fig. 1 details the shapes and dimensions of the samples at various stages of preparation (a) fatigue specimens (b) tomography specimen extracted from the fatigue specimen (c) notch and non-propagating cracks located in the small specimen (d) types of defects and tilting angles.

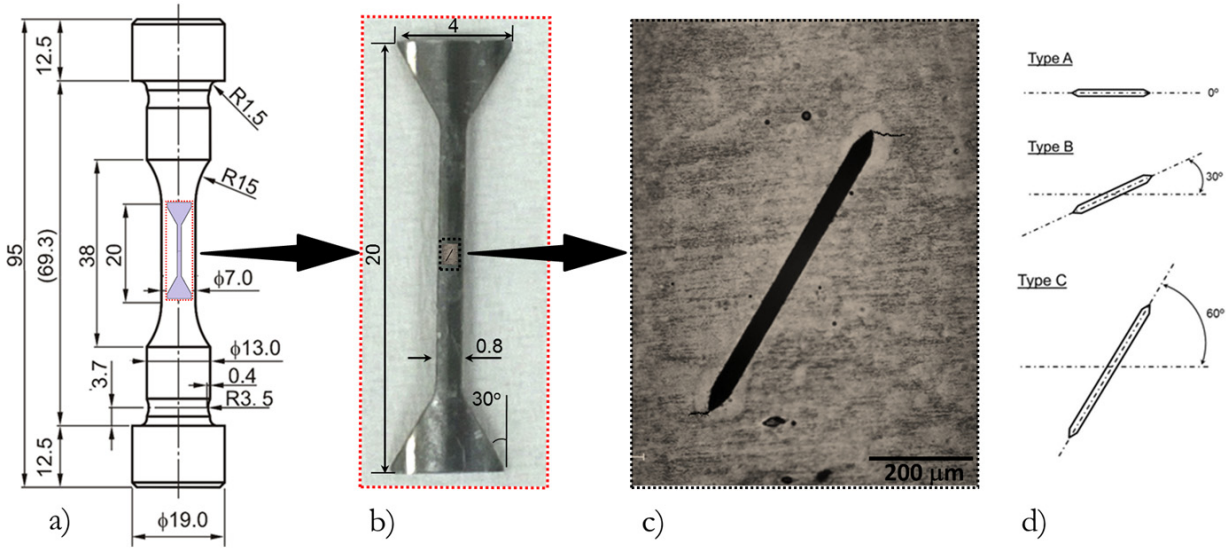


Figure 1: (a) Fatigue specimen (b) tomography specimen extracted from the fatigue specimen (c) notch and non-propagating cracks located in the small specimen (d) types of defects and tilting angles.

## *Synchrotron X-ray microtomography*

The tomography experiments were performed on ID19 beamline at the European Synchrotron Radiation Facility (ESRF) located in Grenoble, France. At it is shown in Fig. 2, a monochromatic X-ray "pink beam" having a photon energy of 60 keV is used. A Pco Edge CCD camera with a 2160 x 2560 pixel chip was used. In order to load the samples for producing crack opening, a dedicated in situ tensile rig was mounted onto the rotation stage of the beamline. 2000 radiographs were taken while the sample was rotating over 180° along its vertical axis; with an exposure time of 0.07 s. (scan acquisition time of 3.68 min). Reconstruction of the tomographic data was performed with a standard filtered back-projection algorithm. A 0.65 µm voxel size was obtained, allowing a good detection of the notch plus cracked areas. Fiji and ParaView open softwares were used for post-processing the images obtaining separately the notch and crack geometries for every steel and defect tilting angle.

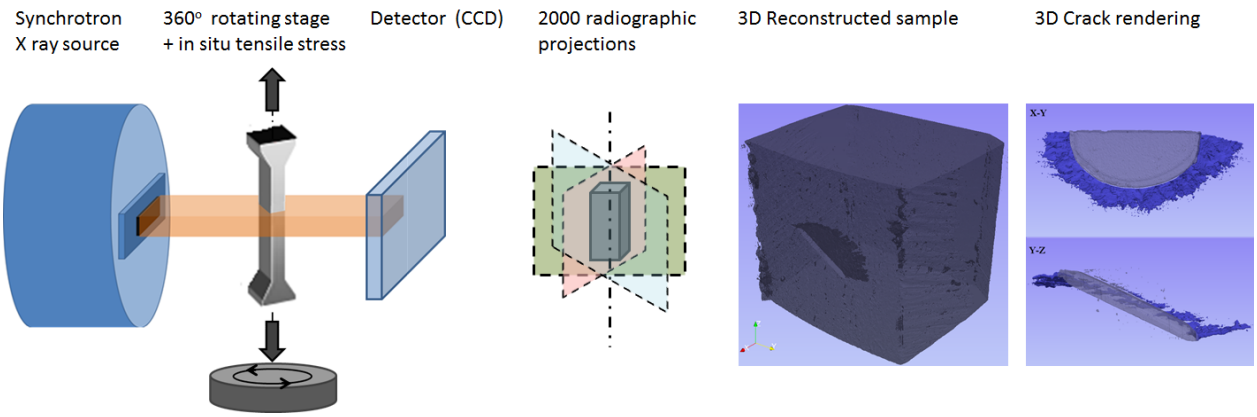


Figure 2: Schematic view of the tomographic acquisition process, volume reconstruction and 3D crack analysis.

## RESULTS

### *3D crack analysis*

A 3D image of the small initiating defect and of the non-propagating fatigue crack was obtained for every defect geometry and steel type. Fig. 3 shows the results in the case of the annealed JIS-S45C steel. Figures on the left show 3D images of non-propagating cracks found at the fatigue limit and figures on the right corresponds to the crack projection (minimum intensity values) in to Z, Y and X planes, Z being the direction parallel to the loading axis.

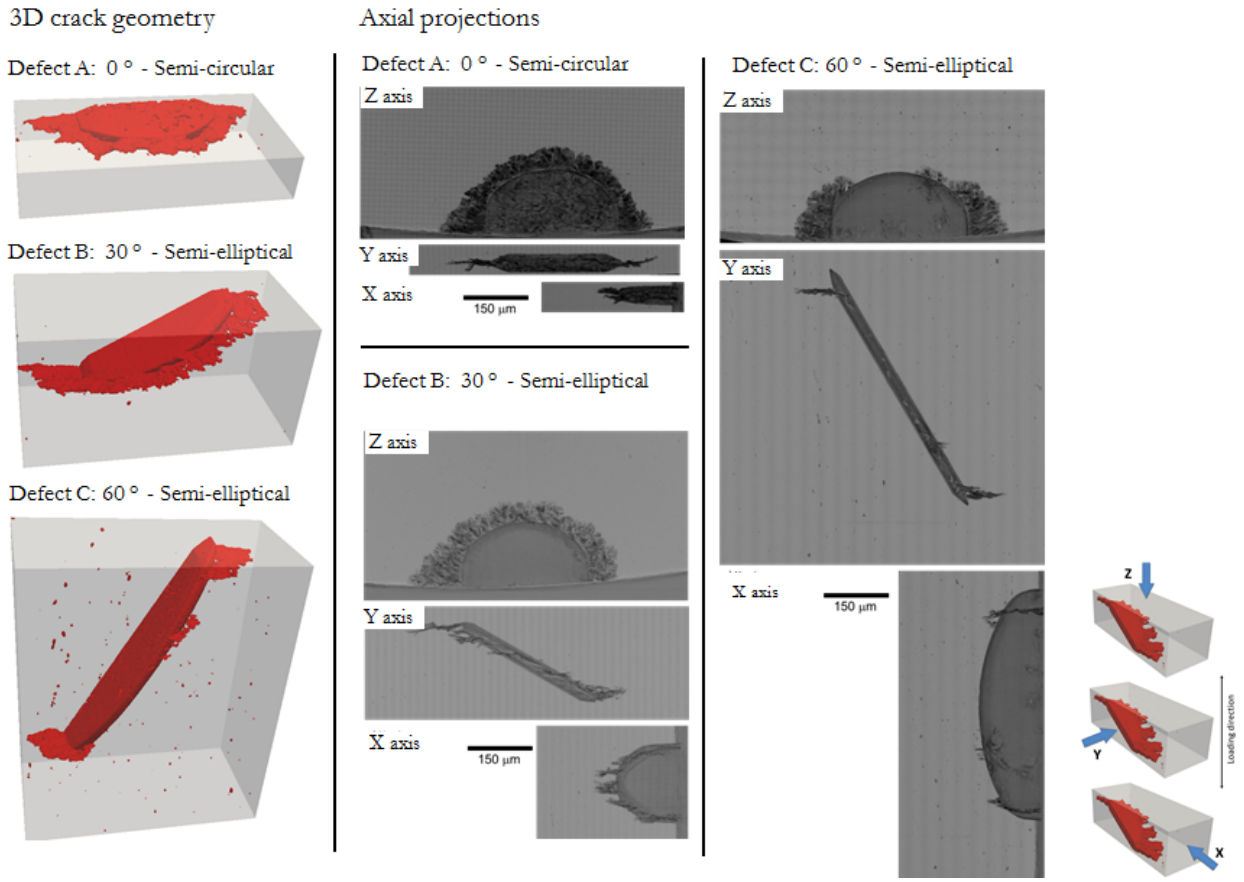


Figure 3: Left: 3D images of non-propagating cracks found at the fatigue limit. Right: Crack projections in to Z, Y and X axis (minimum intensity). Material: Annealed JIS-S45C steel.

| S15C | | | | S45C | | | | SNCM 435 | | | |
|---|---|---|---|---|---|---|---|---|---|---|---|
| O.M. (µm) | 3D (µm) | Diff. (%) | $\sqrt{area}$ (µm) | O.M. (µm) | 3D (µm) | Diff. (%) | $\sqrt{area}$ (µm) | O.M. (µm) | 3D (µm) | Diff. (%) | $\sqrt{area}$ (µm) |
| 652 | 658 | -0.9 | 320 | 497 | 492 | 1.0 | 265 | 356 | 357 | -0.2 | 219 |
| 650 | 655 | -0.8 | 332 | 495 | 515 | -4.0 | 278 | 433 | 440 | -1.6 | 249 |
| 730 | 756 | -3.6 | 334 | 485 | 497 | -2.4 | 252 | 409 | 411 | -0.4 | 226 |

Table 1: Non-propagating crack length measured by Optical microscope (O. M.) and the analysis of 3D images (3D). The $\sqrt{area}$ values were obtained analyzing Z projection images (i.e. Fig. 3 right).

Tab. 1 shows a comparison between the length of non-propagating crack measured at the specimen surface by optical microscope and the surface length obtained by analyzing the 3D images. These measurements are very similar, having a maximum difference of 4 % for the case of S45C steel, 30° notch. Regarding the different materials, the NPC size varied

greatly according to the steel types, i.e. larger non-propagating cracks observed in the softer steel. This observation is consistent with the previous 2D crack analysis performed at the surface in previous work. The $\sqrt{area}$ values corresponding to the square root of the total defect area (notch plus crack) projected on a plane normal to the loading axis are also shown in Tab. 1. These values present the same tendency as the surface length of NPC. These results give confidence in the ability of tomography to measure reliably the length of those small cracks.
From these images it can clearly be seen that longer cracks are always observed at the surface where larger SIF values are found, for every notch tilt angle. In case of the 60° semi-elliptical slit, the crack observed at the notch root seems to be smaller but the projected area of the defect plus crack is similar to those obtained for 0° and 30°. Furthermore in the case of 60° tilted defects, irrespectively of the steel type, cracks do not merge in to a single crack front, propagating in mode I leading to a much more discontinuous front. On the Z projection the NPC presents discontinuities, showing deviations from the typical semi-elliptical single-front shape.

### *FEM mesh reconstruction*

As mentioned before, a calculation of the SIF values for 3D cracks will be helpful for a better understanding of the experimental results. In previous work, a first 2D approach was carried out where the SIFs of two-dimensional cracks were calculated by using finite element analyses and implementing the stress extrapolation method [3]. $K_I$ values where obtained for the different tilt angles and results showed that $K_I$ values of the cracks grown from tilted cracks do not significantly differ from that of non-tilted crack with equivalent projected crack lengths. The maximum difference was about 6% in the crack length range where non-propagating cracks were observed. Of course this is a basic analysis in comparison with the actual notch 3D geometry. In order to extend these results to the 3D field, a FEM analysis including the 3D defect geometry is necessary. As a first step, a FEM mesh of the actual defect was obtained by treating with AVISO software the 3D X-ray images of defects, at it is shown in Fig. 4.

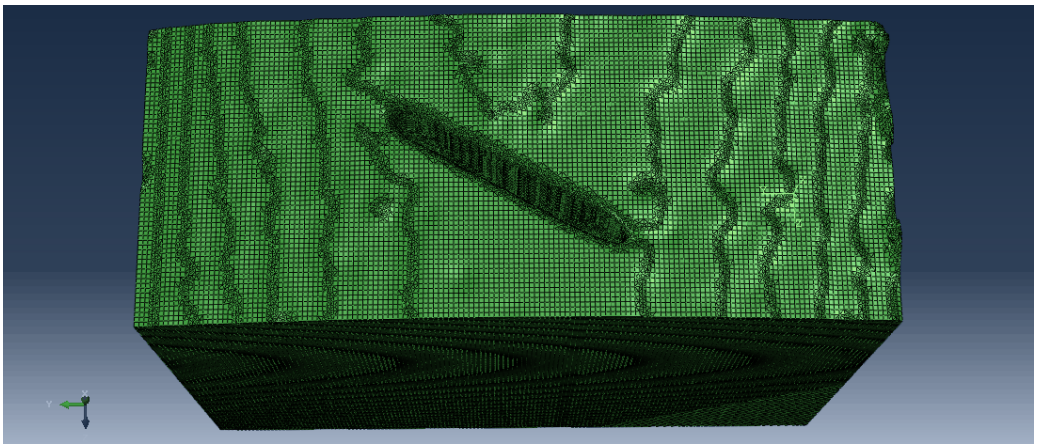

Figure 4: FEM mesh of the actual notch geometry.

This mesh will be a starting point for computing K values near the crack tips for every tilt angle; those values will be used to analyze the 3D shapes of the cracks reported here.

## CONCLUSIONS

High resolution (0.65 μm voxel size) synchrotron tomography was used to obtain 3D images of arrested cracks initiated from artificial defects in 3 different steels.
Good contrast level between crack and bulk facilitates accurate measurements. Surface crack length measured by this technique gave the same results as optical microscope measurements.
The $\sqrt{area}$ values present the same tendency as the surface length of NPC, i.e. larger non-propagating cracks were observed in the softer steel.
In the case of 60° tilted defect, the crack fronts appear much more discontinuous with several cracks propagating in mode I until arrest.

3D imaging allowed us to generate FEM mesh that will be used to perform 3D FEM calculation of SIFs values for more detailed analysis.

## REFERENCES

[1] Lorenzino, P., Okazaki, S., Matsunaga, H., Murakami, Y., Effect of orientation of small defects on fatigue limit of steels, Web of Conferences. EDP Sciences, 12 (2014).
[2] Murakami, Y., Metal Fatigue: Effects of Small Defects and Nonmetallic Inclusions, Elsevier Ltd., Oxford, UK, (2002).
[3] Lorenzino, P., Okazaki, S., Matsunaga, H., Murakami, Y., Effect of small defect orientation on fatigue limit of carbon steels, FFEMS, under review, (2015).